Agha Inya Ndukwe, Justus Uchenna Anaele*

CORROSION OF DUPLEX STAINLESS-STEEL WELDMENTS: A REVIEW OF RECENT DEVELOPMENTS

KOROZIJA DUPLEKS NERĐAJUĆIH ČELIKA: PREGLED SKORIH ISTRAŽIVANJA

Originalni naučni rad / Review paper
UDK /UDC:

Rad primljen / Paper received: 2.03.2023

Adresa autora / Author's address:
Department of Materials & Metallurgical Engineering, Federal University of Technology, Owerri, Imo State, Nigeria *email: agha.ndukwe@futo.edu.ng

Keywords
- corrosion
- duplex stainless steel
- weldment
- pitting
- welding

Ključne reči
- korozija
- dupleks nerđajući čelik
- zavareni spoj
- piting
- zavarivanje

Abstract

This work covers the review of previous studies on the corrosion of welded joints of duplex stainless steel (DSS) from 2015-2022. DSS alloys have been welded using a variety of processes including laser fibre, gas tungsten arc, shielded metal arc, and underwater flux-cored arc welding. The predominant corrosive media these welded joints were subjected to in corrosion studies were NaCl (1 M), ferric chloride (6 %), $MgCl_2$ (45 wt.%), HCl (1 M), and H_2SO_4 (2 M). The reported results revealed that the Mo concentration in hyper-duplex stainless steel was shown to not affect weldment corrosion; rather, low pitting resistance equivalent number (PREN) austenite regions and austenite-ferrite grain boundaries were prone to pitting and intergranular corrosion. The material's stir (friction) welded joint (S32750) was reported to have the best corrosion resistance in NaCl (1 M). The weldment of the DSS joint generated by gas tungsten arc welding was found to be more resistant to pitting than that produced by shielded metal arc welding.

Izvod

U radu je dat pregled prethodnih istraživanja o koroziji zavarenih spojeva od dupleks nerđajućih čelika (DSS), od 2015-2022. Legure DSS su zavarene primenom raznih postupaka, uključujući lasersko, TIG, obloženom elektrodom, kao i podvodnim elektrolučnim zavarivanjem punjenom žicom. Dominantne korozivne sredine kojima su tretirani ovi zavareni spojevi bile su NaCl (1 M), ferihlorid (6 %), $MgCl_2$ (45 tež.%) i H_2SO_4 (2 M). Dobijeni rezultati pokazuju da koncentracija molibdena u hiper-dupleks nerđajućem čeliku ne utiče na koroziju zavarenog spoja; zapravo, niska vrednost pokazatelja ekvivalenta otpornosti prema piting koroziji (PREN) oblasti austenita i austenitno-feritne granice zrna su bile podložne pitingu i interkristalnoj koroziji. Najbolju otpornost prema koroziji u NaCl (1 M) pokazao je zavareni spoj (S32750) dobijen zavarivanjem trenjem sa mešanjem. Zavareni spoj DSS dobijen zavarivanjem TIG postupkom pokazao je veću otpornost prema pitingu u odnosu na spoj dobijen zavarivanjem obloženom elektrodom.

INTRODUCTION

Duplex stainless steels (DSS) consist of commensurate proportions of face-centred cubic (austenite) and body-centred (ferrite) with minimal content (less than 0.03 wt.%) of carbon. They are fundamentally rooted in the Fe-Cr-Ni system with 4-8 % Ni, and 20-30 % Cr compositions, /1-2/. On the other hand, Super duplex stainless steels (SDSS) are dual-phase alloys with ferrite and austenite volume fractions as near to 50/50 as feasible at room temperature. Despite the good mix of characteristics, SDSS can suffer from hydrogen embrittlement, /3/.

Many issues have been connected with the welding of duplex stainless steels; however, attempts are being made to determine the optimal parameters and chemical combinations that can result in great welds. Duplex stainless steels offer stronger resistance to crevice and pitting corrosion than conventional austenitic stainless steels and may resist chloride-induced stress-corrosion cracking /1/. This is true owing to the inclusion of larger levels of C, Cr, Ni, and Mo than the typical austenite stainless steel /5/. Electrochemical impedance spectroscopy (EIS) has recently been widely used to understand the mechanism of corrosion behaviour in stainless steel /4/. The research to evaluate corrosion behaviour of a stir (friction) welded DSS joint indicates that the corrosion resistance of the weld was higher than that of the underlying material, and it increased as the heat input increased, /6/.

New operational requirements of many oil and gas sectors have necessitated unprecedented improvement in the production of highly corrosion-resistant alloys /7/. Since the early 1980s, the use of DSS in the oil and gas sector has geometrically increased owing to their exceptional resistance to pitting in chloride-based media, and appreciable toughness at low temperatures /8/. Bilyy et al. /9/ acknowledged that the combination of strength and effective corrosion resistance has made DSS stand out above stainless steels that are majorly austenitic or ferritic. These excellent features exhibited by DSS hinge on the microstructure, and satisfactory balance of the constituent alloying elements including heat treatment /10/. In essence, DSS can serve as a preferred alternative to either austenitic- or ferritic-based stainless steel /11/.

Several aspects of the welding process have been identified to influence pitting corrosion resistance. These features are not limited to /1/:

i. root pass nitrogen loss, and
ii. the manifestation of a certain degree of degradation at the underside of the root head.

The degree to which corrosion resistance is reduced is determined by which of these factors is active and to what extent, /1/.

GRADE DESIGNATION AND CORROSION OF DUPLEX STAINLESS STEEL WELDMENTS

Development and grade designation of DSS

The first manufactured common duplex stainless steel has been reported to consist of Ni (3-4 %), Cr (25 %), and Mo (1.5 %) and is referred to as type 329 (S32900). When welded, however, this grade loses its optimal balance of austenite and ferrite, reducing corrosion resistance and toughness /1, 12/. Advances in technology, aimed at remedying the situation led to the introduction of nitrogen in stainless steel through the argon-oxygen decarburization technology. By this development, the introduced nitrogen increased the formation of austenite from the ferrite, even at an elevated temperature to ensure that the acceptable proportions of ferrite-austenite components are maintained within the heat-affected zone after completing the welding process, /13/.

Duplex stainless steels have three fundamental forms including super duplex (high-alloy), intermediate (medium-alloy), and low-alloy grades. The relationship /14/ may be used to characterize duplex stainless steels based on their pitting resistant equivalent number with nitrogen (PREN):

$$\text{PREN} = \%\,\text{Cr} + 16 \times (\%\,\text{N}) + 3.3 \times (\%\,\text{Mo}). \quad (1)$$

If by any means, the element W is made to be a constituent material in the duplex stainless steel, the accompanying PREN equation becomes /1/:

$$\text{PREN-W} = \%\,\text{Cr} + 0.5\times\%\,\text{W} + 16\times(\%\,\text{N}) + 3.3\times(\%\,\text{Mo}) \quad (2)$$

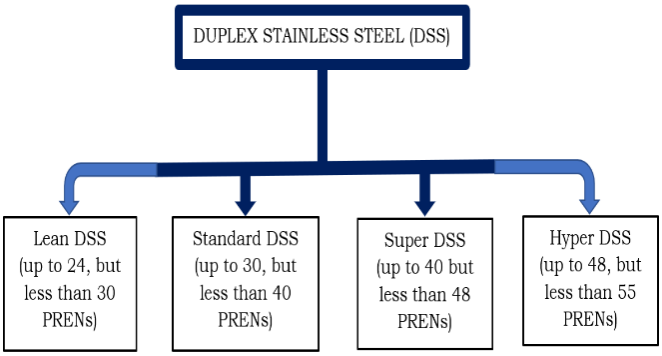

Figure 1. Schematic illustration of the categorization of DSS based on their PREN, /14-15/.

According to Francis and Byrne /15/, different types of duplex stainless steels (Fig. 1) may be categorized based on the PREN including hyper DSS (up to 48, but less than 55 PREN), super DSS (up to 40 but less than 48 PREN), standard DSS (up to 30, but less than 40 PREN), and lean DSS (up to 24, but less than 30 PREN). It is worth of mention that these classes of DSS can have different characteristics, but they possess a shared morphology of commensurate austenite and ferrite proportions, /5/.

Prediction of weld metal structure

The weld metal structure of DSS material can be predicted using the Welding Research Council (WRC) - 1992 constitution diagram /62-63/. WRC -1992 constitution diagram was developed from manual metal arc weld metal and applies to common arc welding processes /62/. Predictions can be made for a particular composition by categorizing alloying elements as 'ferrite stabilizing' (such as Cr, Mo, Si, Nb) or 'austenite stabilizing' (such as Ni, Mn, C and N) and calculating the 'Cr and Ni equivalents' which are then plotted on the Fe-Cr-Ni equilibrium diagram /64/. The concept of Ni equivalent (Ni_{eq}) is the term used for cumulative effects of austenite stabilizing elements as a weighted summation of their respective concentration levels. On the other hand, Cr equivalent (Cr_{eq}) is the term used for cumulative effects of ferrite stabilizing elements as a weighted summation of their respective concentrations, /62/.

The weld metal structure is better understood by referring to Fe-Cr-Ni equilibrium diagram /65/. From the Fe-Cr-Ni equilibrium plot /65/, it can be seen that the composition of DSS lies within the $\alpha + \gamma$ phase region. DSS have high corrosion resistance due to a balanced austenite-ferrite microstructure, /75/. Austenite structures are formed in the weld under conditions when $Cr_{eq}/Ni_{eq} < 1.5$ and there is no further change in the structure after solidification. The duplex structure is formed in the weld metal under the condition when $Cr_{eq}/Ni_{eq} \approx 1.5$-$1.6$. Fully ferritic weld metal structures are formed under the condition when $Cr_{eq}/Ni_{eq} > 1.9$, /66/. However, studies have shown that the base metal of DSS has Cr_{eq}/Ni_{eq} in the range of 2.25-3.5, /62/. Cr_{eq}/Ni_{eq} for 2507 DSS and 2205 DSS are 2.25 and 2.62, respectively, and is attributed to the high diffusivity of Cr and Mo in the ferrite phase, /62/.

Corrosion behaviour of DSS weldments

It has been found that the heat-affected zone (HAZ) of welded duplex stainless steel is more prone to deterioration /1, 16/. Figure 2 depicts a schematic representation of the heat-affected zone formed by gas tungsten arc welding. The situation has been identified to be caused by the unproportionate balance of ferrite/austenite fractions.

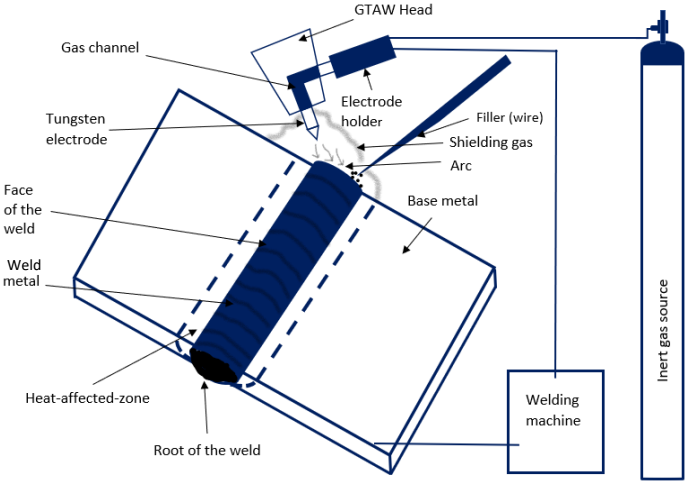

Figure 2. Schematic illustration of the HAZ produced by gas tungsten arc welding, /17-18/.

Resistance to pitting corrosion of duplex stainless-steel weldment is affected by the cooling rate and applied heat during the welding process. In essence, the resistance to pitting corrosion can be enhanced by a slow cooling rate and higher heat input as indicated in Fig. 3a.

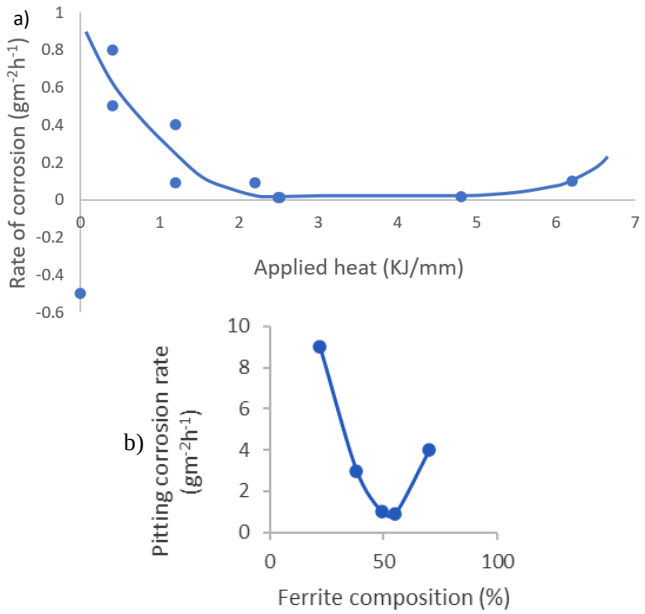

Figure 3. Schematic representation of the effects: a) applied heat on the corrosion of duplex stainless steel (S31803) welded in a ferric chloride-containing solution; and b) approximations of austenite-ferrite proportions on the resistance to pitting of duplex stainless steel (Fe-22Cr-5.5Ni-3.0Mo-0.12N), /1/.

Optimal corrosion protection (see Fig. 3b) can be achieved by ensuring that the welding process engenders approximately equal austenite and ferrite proportions in both the weld metal and HAZ /1, 16/. Slowing the cooling rate, high heat input, pre-heating in multi-pass welding operations, and controlled inter-pass temperatures can all help to achieve a balanced ferrite/austenite composition. Constituent alloying elements in duplex stainless steels play a major part in influencing corrosion properties, /19/. It is worthy of note that the duplex stainless steel has immeasurable resistance to elevated temperature oxidation. But it is susceptible to carbon precipitation including the formation of chromium nitrite (Cr_2N) and chromium nitride (CrN) phases. This anomaly can be resolved by employing solution annealing and welding procedures under strict control, /1/.

At prolonged exposure to high temperatures (between 300 and 1000 °C), duplex stainless steels of a ferritic matrix with high alloy content are prone to embrittlement and degradation of toughness. The reason for this behaviour is attributed to the precipitation of several intermetallic phases, /1/.

OVERVIEW OF RECENT STUDIES ON THE CORROSION OF DSS WELDED JOINTS

Recent studies on the corrosion of DSS welded joints under various conditions are evaluated and reported in this section. The summary of findings occasioned by research relevant to the understanding of the corrosion of DSS weldments resulting from different factors can be summarized in Table 1.

Table 1. Summary of relevant investigations on the corrosion of duplex stainless-steel welded joints.

Welded material	Welding technique used	Wire (filler) material used	Corrosion study method employed	Corrosive solution used	Comments on weldment corrosion resistance	Ref.
DSS (2205)	GTAW	Electr. (0.024 C, 0.72 Si, 0.80 Mn, 0.016 P, 0.019 S, 22.22 Cr, 9.36 Ni, 3.01 Mo, 0.06 Nb, and 0.154 wt.% N, bal. Fe)	PDP	NaCl (3.5 wt.%)	As the HAZ and base metal were separated by more space, the susceptibility to corrosion steadily reduced.	/20/
ASS (316L) and DSS (2205)	GTAW	AWS ER 309L, AWS ER 347, and AWS ER 316L	EIS & PDP	NaCl	The electrode AWS ER 309L was found to offer excellent corrosion resistance to the weldment.	/21/
DSS 2205 (UNS S31803)	Laser (fibre) with nitrogen and argon as shielding gases	-	PDP	NaCl (3.5 wt.%)	The weldment's resistance to corrosion was improved by the presence of N.	/22/
LDSS (UNS S82441)	Stir (friction)	Polycrystalline cubic boron nitride (PCBN) with 40% W and 25% Re.	PDP	NaCl (0.6 M)	The austenitic region was found to be more resistant to localized corrosion than the ferritic phase.	/23/
DSS (2205)	SMAW and GTAW	E2209 and E2209	G48 (ASTM) method (A)	100 grams of ferric chloride, $FeCl_3.6H_2O$, and 900 millilitres of deionized water	At 850 °C, there were significant concentrations of intermetallic phases inside the matrix, which caused severe pitting corrosion and the most metal loss. Since total dissolving occurred at 1050 °C, no pitting corrosion was seen there.	/24/
DSS (UNS S32101)	(FCAW-136) undersea flux-cored arc welding, both dry and wet.	ER2209	DL-EPR	HCl (0.1%) + H_2SO_4 (33 %)	In comparison to the heat-affected zone, the weld metal demonstrated greater resistance to localized corrosion.	/25/

DSS (2205)	EBW	-	PDP & DL-EPR	NaCl (3.5 %)	The weldment produced using the electron beam welding method had a substantially greater vulnerability to pitting corrosion than the base metal.	/26/
DSS (UNS S31803)	MAG/MIG short circuit procedure	ER2209	PDP	NaCl (1 M)	When the welding circumstances were compared, the intergranular corrosion resistance was unaffected.	/27/
DSS (2205)	GTAW (Numerous-pass)	ER- 2209	DL-EPR	HCl (1.5 M) + H_2SO_4 (2 M)	During multi-pass welding, chromium nitride precipitation decreased the DSS joint's intergranular corrosion resistance.	/28/
DSS (2507)	Stir (friction)	-	EIS & PDP	NaCl (3.5 wt.%)	The stir zone had greater corrosion resistance than base metal because the refined grains in the stir zone enhanced element diffusion and increased the passivation coating's longevity.	/29/
DSS (2205)	Wet flux-cored arc welding in the water (FCAW)	Self-shielded flux-cored wire based on Ni (2.7% Mn, 3%Cr, 35.9%Ni, and 56.6%Fe)	PDP	NaCl (3.5 wt.%)	Corrosion resistance of the weld was found to be greater under high heat input, but inferior to that of the base material.	/30/
DSS (2205)	GTAW	AWS E2209-16	G48 (ASTM) method (A)	Ferric chloride (6 %)	When tested at 22 °C using the ASTM G48 Method A, no pitting was found in all of the test samples.	/31/
DSS (2205)	TIG & ATIG	ER2209	G36 (ASTM)	MgCl2 (45 wt.%) at 155 °C	Regardless of used welding techniques, the resistance of joints to stress corrosion cracking was lower than that of base metal.	/32/
DSS (2205)	GTAW	ER2209	G48 (ASTM) method (A)	FeCl3 (6 wt.%) at 35 °C	Ageing treatments deteriorated pitting resistance, with the highest loss found correlating to thermal ageing at 850 °C per 2 h.	/32/
SDSS (825/UNS S32750)	GTAW	ER347	PDP & EIS, G106 (ASTM)	NaCl (1 M)	The root passes of the weldments were more susceptible to pitting corrosion than the cap passes.	/34/
SDSS (UNS S32750)	SMAW	E2595	DL-EPR	NaCl (3.5%)	For both heat inputs, applied in the study, the ferrite concentration was greater in the weld zone than in the base metal.	/35/
SDSS (UNS S32750)	Laser (pulsed)	Nickel thin foils	G150-18 (ASTM)	(1 M) NaCl	The prevalence of ferrite hampered the corrosion resistance of the HAZ, which was the site of pitting.	/36/
DSS (2205)	SMAW	ER2205	G150-1999 (ASTM)	Ferric chloride medium	In the coarse-grained heat-affected zone close to the weld joint's fusion line, pitting corrosion easily developed.	/37/
DSS (2101)	(FCAW) Hyperbaric under-sea flux-cored arc welding	Lincoln Supercore 2205P flux-cored wire with UNS 32101 DSS	DL-EPR	HCl (1 M) + H_2SO_4 (2 M)	It was found that the weld's root zone had more significant corrosion than the middle zone.	/38/
DSS (UNS S32304)	SMAW	AWS A5.9 ER2209	PGSTAT 100 potentiostat by Autolab.	NaCl (1 M)	Cold wire addition decreased the dilution of the weld metal and improved its corrosion resistance, while significant ferrite fractions led to pitting in HAZ.	/39/
DSS	Stir (friction)	-	G61-94 (ASTM), Cycle-dependent potentiodynamic polarization	H_2SO_4 (0.1 M) + NaCl (0.1 M)	Number of pits increased but the size of the pits shrunk as a result of the faster welding pace.	/40/

UNS S32205 (DSS)	MIG	ERCrNiMo-3	PDP	NaCl (3.5 wt.%)	When compared to the weld metal root, the corrosion rate at the weld metal face increased due to the precipitation of intermetallic phases.	/41/
HDSS	(FCAW	-	PDP & DL-EPR	HCl (1.5 M) + H2SO4 (2 M) & NaCl (3.5 wt.%)	Within the austenitic area with low PREN, pitting was seen.	/42/
SDSS & DSS (UNS S32101, S32760, S32205, and S32750)	Stir (friction)	-	A923 (ASTM), WL, Cycle-dependent potentiodynamic polarization	NaCl (1 M)	With S32101 DSS, a lower weldment corrosion resistance was found.	/43/
LDSS (UNS 32101)	GTAW	ER2209	EIS & PDP	NaCl (3.5%)	The low heat input was discovered to be beneficial to the weld metal high corrosion resistance.	/44/
2205 DSS	electron beam (EB) welding process	-	Electrochemical methods	3.5 % NaCl solution and 2 M H_2SO_4 + 0.01 M KSCN + 0.5 M NaCl	Precipitate formation in the ferrite matrix of the fusion zone acted as nucleation sites for pitting corrosion, especially in the root region of the weld	/58/
UNS S32304 DSS	SAW	Cold stainless steel wire	Electrochemical method	corrosive chloride medium	It is observed that the weldments produced from welding heat input greater than 2.7 kJ/mm exhibited better corrosion properties compared to weldments produced from low heat input (≤ 2.5 kJ/mm).	/67/
UNS S32101 DSS	Keyhole-TIGW	-	Electrochemical method	Sodium chloride solution	Corrosion resistance of the weldments increases with heat input due to increased ferrite-to-austenite transformation with increasing welding heat input	/60/
UNS S32205 DSS	TIGW	ER-2209 filler wire	cyclic polarization and electro-potential tests	NaCl 3.5wt.% solution	Crevice corrosion of DSS weld metal is initiated at grain boundaries and progresses by choosy corrosion of the susceptible phases	/59/
2205 DSS	GMAW	ER 2209 filler wire	Electrochemical method	Artificial seawater and H_2S gas media at 70 °C	Pitting corrosion of DSS weld metal is sensitive to the evolved microstructures. Corrosion occurred by mechanisms of grain boundary pit formation and crack propagation	/61/
AISI 2205 DSS	SMAW	Variable electrodes	Potentiodynamic polarization test	3.5% NaCl solution	Pitting corrosion is reported to occur by mechanisms of chromium depletion and precipitation of chromium nitride at ferrite-austenite boundaries	/54/
UNS S32205 DSS	GMAW process	ER2209 filler	ASTM A262 and ASTM G48 practice A	ASTM A262 and ASTM G48 practice A	HAZ of joints produced with high heat input (3.5 kJ/mm) has characteristic coarse austenite grain structures and were found to be more prone to intergranular corrosion along ferrite-austenite boundaries compared to 0.5 kJ/mm and 1.0 kJ/mm joints.	/75/

Geng et al. /20/ in their study evaluated the impact of the welding process (GTAW) on the corrosion and microstructural behaviour of DSS (2205). The weldment was exposed to a solution containing NaCl (3.5 %) at room temperature. The weldment was categorized into zones to make for adequate corrosion studies. It was reported that pitting was more severe in zone 2, which consisted of austenite (23.05 wt.% Cr, 3.19 wt.% Mo, and 7.71 wt.% Ni) and ferrite (24.58 wt.% Cr, 3.77 wt.% Mo, 5.34 wt.% Ni). In other words, degradation was higher as the base metal was approached.

The existence of a higher volume composition of the ferrite phase, the precipitation of the Cr_2Ni phase, and the bigger grain size of ferrite relative to other phases were thought to be the causes of the strong pitting attack seen in zone 2 /20/. The resistance to corrosion of welded joints made of duplex stainless steel (2205) and austenitic stainless steel (316L) in NaCl was researched by Moteshakker et al. /21/. They used different welding electrodes, including AWS ER 309L, AWS ER 316L, and AWS 347. It was concluded that the weldment produced with wire AWS ER 347 encouraged the formation of the chromium nitride phase, thereby leading to decreased resistance to corrosion, whereas electrode AWS ER 309L was found to exhibit excellent corrosion resistance of the welded dissimilar alloys.

Ma et al. /29/ conducted a study to improve the corrosion resistance of DSS (2507) using stir friction welding technique. According to the findings of electrochemical experiments, pitting corrosion mostly happened at the boundary between ferrite and austenite phases or in the ferrite phase, where there is low PREN. On the other hand, the refined grains in the stir zone boosted element diffusion and increased the durability of passivation coating, resulting in superior corrosion resistance of the stir zone than the base metal /29/. In another research, the arc welding (wet flux-cored underwater) technique was used to weld DSS (2205) with a nickel-based filler /30/. The results indicated that the corrosion resistance of the weldment was lower than that of the weld metal under three heat inputs (23.5, 32, and 16.9 kJ/cm), although it improved as heat input increased. Corrosion resistance of the weldment was found to be greatest at 32 kJ/cm.

Nanavati et al. /31/ investigated the ferrite composition of the weldment to unravel its stress corrosion cracking behaviour when exposed to ferric chloride (6 %). They concluded that after 1000 h exposure time, no stress corrosion cracking was seen. Alwin et al. /32/ on the other hand, studied the effect of tungsten gas welded DSS (2205) on the stress corrosion cracking (SCC) of the weldment. The SCC test was conducted in a magnesium chloride solution at approximately 155 °C. It was reported that no matter the nature of the welding process employed, the base metal offered superior resistance to stress corrosion cracking than the weld joint. On the other hand, the welded joint obtained by tungsten inert gas (TIG) welding technique was found to be inferior to the welded joint produced by activated tungsten inert gas (ATIG) welding. The reason for this development was credited to grain growth and lack of commensurate ferrite-austenite balance of the welded region.

Singh et al. /33/ studied the influence of ageing on the corrosion resistance of the DSS weldment. They conducted some isothermal heat treatments that spanned from 475 to 1050 °C. It was reported that in the as-welded condition, the welded joint had the strongest resistance to pitting corrosion. The ageing heat treatment generated degradation in the pitting resistance behaviour of the weldment, and the highest loss observed corresponded to the thermal ageing at 850 °C per 2 h. In general, the base metal outperformed the weld metal in terms of pitting corrosion resistance. Kangazian et al. /34/ worked on the influence of applied pulse current on the corrosion of SDSS (825/UNS S32750) welds. Welding was carried out using continuous current and pulse current methods. They reported that pulsed current was better than the continuous method, hence, it enhanced the resistance to pitting. A study to investigate how the corrosion rate of SDSS (UNS S32750) is influenced by heat input has been undertaken, /35/. Two heat inputs 1.10 and 0.54 kJ/mm were used in the study. The corrosion studies in NaCl (3.5 %) solution revealed that the magnitude of sensitization was less than 1 % and there was no significant difference in pitting potentials for the two heat inputs. Furthermore, Da Cruz Junior /36/ investigated the resistance to corrosion of the SDSS weldment (UNS S32750) produced by laser welding. The corrosion study was carried out in (1 M) NaCl. It was discovered that the heat-affected zone was susceptible to pitting. The reason was attributed to the predominance of the ferrite phase within the heat-affected zone.

Wu et al. /37/ studied pitting resistance when the DSS (2205) welded joint was exposed to a ferric chloride solution. The heat-affected zone was discovered to be prone to pitting owing to the presence of coarse-grained constituent phases. In another study, the impact of microstructure on the resistance to corrosion of DSS (2101) weldment was undertaken /38/. They observed that the precipitation of Cr_2N particles within the heat-affected zone makes it more prone to corrosion than the base material. Atapour et al. /40/ probed the vulnerability of the welded joint of DSS to pitting. They reported that the reduction in heat input can lead to a reduction in the enlargement growth of pits in the weldment. Another study investigated how the cold wire feeding rate and different applications of heat can affect pitting corrosion of a welded DSS (UNS S32304). It was reported that pits were more prevalent in the HAZ than the base metal. This development was said to be caused by the presence of chromium nitride and an increased fraction of ferrite.

Tümer et al. /41/ studied the corrosion disposition of DSS (UNS S32205) with different weldments in the presence of NaCl (3.5 wt.%). It was reported that the face of the weld metal was most vulnerable to corrosion while the root of the weld metal was most resistant to corrosion. The presence of some precipitated intermetallic phase within the weld face was attributed to cause degradation. In another study, Kim et al. /42/ investigated how the presence of molybdenum in duplex stainless steel (hyper) can influence corrosion resistance of the weldment. The results reveal that the austenite-ferrite grain boundaries were vulnerable to intergranular corrosion. It was also indicated that the austenitic region with low PREN exhibited pitting irrespective of the molybdenum content. Santa Cruz et al. /43/ studied the resistance to corrosion of both super-duplex and duplex stainless steel (UNS S32750, S32760, and S32205) weldments obtained by stir (friction) welding. The corrosive medium used was NaCl (1 M) solutions. Results reveal that the weldment of the material S32760 exhibited lower resistance to corrosion in NaCl (1 M) medium. In addition, the heat-affected areas within the austenite-ferrite grain boundaries suffered higher corrosion rates than the base metal. For the S32750 material, the base metal and the weldment shared a similar optimal resistance to corrosion in NaCl (1 M) solution. Ouali et al.

/44/ investigated how microstructure and heat inputs (1.05, 0.98, and 1.20 kJ/mm) can affect the corrosion resistance of lean duplex stainless steel (LDSS), UNS S32101. They reported that the resistance to pitting corrosion of the LDSS weldment decreased with increase in applied heat. The reason for this outcome was attributed to the reformation of austenite (secondary) with minute traces of Mo, N, and Cr content within the weldment.

Hou et al. /55/ studied the corrosion mechanism in HAZ of duplex stainless steel (DSS) weld metal. The study observed that the HAZ experienced high temperatures with characteristic ferrite single-phase microstructure which is susceptible to pitting corrosion. It was explained that pitting corrosion occurs by mechanisms of Cr depletion at the vicinity of Cr nitride and precipitation of intermetallic (Ti, Cr)N in the ferrite matrix of HAZ of DSS weld metal. In a related study, Shen et al. /57/ confirmed that the HAZ of a DSS weld metal is prone to pitting corrosion due to the precipitation of chromium nitride and the formation of austenite in the high-temperature region of HAZ. Singh et al. /58/ studied corrosion behaviour of weld fusion zone 2205 DSS material produced by electron beam (EB) welding. Electro-potential methods were used to determine pitting corrosion rates. The propensity for pitting corrosion is observed to be higher in the weld metal fusion zone compared to the DSS base metal. This was attributed to the lack of homogenous microstructure associated with the fusion zone. Precipitate formation in the ferrite matrix of the fusion zone acted as nucleation sites for pitting corrosion, especially in the root region of the weld. These studies suggest that weld metal microstructure may be employed to control the corrosion of DSS weldments. Santos et al. /67/ studied the corrosion of UNS S32304 DSS weldment produced by submerged arc welding (SAW) using cold wire filler. Weldments produced from varied welding heat inputs were exposed to a corrosive chloride medium, and corrosion rates were measured and recorded. It is observed that weldments produced from welding heat input greater than 2.7 kJ/mm exhibited better corrosion properties compared to those produced from low heat input, ≤ 2.5 kJ/mm. High corrosion resistance observed with weldments produced from high heat input was attributed to the formation of relatively lesser precipitates and a higher volume fraction of the austenite phase in the weld metal. It was explained that more precipitates are formed with low welding heat input and these precipitates act as nucleation sites for the corrosion of DSS weld metal. This result agrees with the postulations of Calderon-Uriszar-Aldaca et al. /68/, Chen et al. /69/, and Zhang et al. /73/ where it was stipulated that austenite structures in DSS weld metal (in chloride medium) exhibited higher resistance to pitting and crevice corrosion compared to weldments dominated with ferrite phases. Cui et al. /60/ studied the microstructure and corrosion behaviour of UNS S32101 DSS welded joints produced by keyhole tungsten inert gas welding. Different samples of welded joints were produced by varying the heat input (1.99, 2.14, 2.30, and 2.46 kJ/mm). Various weld metal samples were exposed to a corrosive medium containing 1 M per litre concentration of sodium chloride solution at ambient temperature and corrosion rates were measured using electrochemical methods. It is observed that the volume fraction of the austenite phase in the weld metal fusion zone is greater than the austenite content of HAZ for a given heat input. This observation suggests that the weld metal fusion zone exhibits more resistance to pitting corrosion than the HAZ. It is also observed that the corrosion resistance of weldments increases with heat input due to increased ferrite-to-austenite transformation with increasing welding heat input. Fusion weld metal zones and HAZ were characterized by the precipitation of chromium nitrides (CrN and Cr_2N) within duplex structures and these precipitates served as nucleation sites for pitting corrosion. These precipitates were observed to decrease with an increase in welding heat input and were not present at a high heat input of 2.46 kJ/mm. The study concludes that the optimal welding heat input for maximum pitting corrosion resistance in DSS weldments is therefore 2.46 kJ/mm. Nunez de la Rosa et al. /59/ studied corrosion behaviour of UNS S32205 DSS welded joint produced by tungsten inert gas welding (TIG). ER-2209 filler wire was used with welding current and voltage in the ranges of 110-200 A and 23-28 V, respectively. The DSS base material and DSS weldments were exposed to a corrosive medium containing NaCl 3.5 wt.% solution at room temperature and the corrosion rates were determined by cyclic polarization test (for pitting corrosion) and electro potential test (for crevice corrosion). It is observed that the inert film produced on the base material was more shielding compared to that on the DSS welded joints. However, the microstructure of the DSS weld metals was not susceptible to pitting corrosion due to the absence of carbide and nitride intermetallic compounds and balanced austenite-ferrite phases. It is observed that crevice corrosion of DSS weld metal is initiated at grain boundaries and progresses by choosy corrosion of susceptible phases. This observation has been reported by Torress et al. /74/ and Calabokis et al. /71/ where it was confirmed that crevice corrosion of 25Cr DSS and UNS S32750 DSS, respectively, originates at grain boundaries. Miranda-Pérez et al. /61/ studied the corrosion of 2205 DSS welded joints produced by gas metal arc welding (GMAW). Three different weld metal sample categories were produced at various welding heat inputs (0.616, 0.516, and 0.437 kJ/mm) using ER 2209 filler wire. Weld metal samples were exposed to artificial seawater (composed of 250 g of NaCl and 25 g of CH_3COOH in 4725 mL of distilled water) and hydrogen sulphide gas media at 70 °C, and corrosion rates were determined. The study noted that the pitting corrosion of DSS weld metal is sensitive to the evolved microstructures. Weld metal microstructures were characterized by grain boundary austenite (GBA), partly transformed austenite (PTA), Widmanstätten austenite (WA), intergranular austenite (IGA) and ferrite phases. Corrosion of DSS weld metals was explained to occur by two major mechanisms:

- formation of micro pits in grain boundaries and within susceptible phases such as ferrite matrix,
- crack initiation and propagation within Widmanstätten austenite and intergranular austenite.

It is observed that the resistance to pitting corrosion in DSS weldments increases with heat input.

Omiogbemi et al. /54/ studied corrosion characteristics of AISI 2205 DSS weld metal produced by a shielded metal arc welding process with varied welding parameters. The corrosion studies on welded joints were carried out in a 3.5 % NaCl solution, and a potentiodynamic polarization test was used to determine the corrosion rates of the weldments. It is observed that chloride radicals from a corrosive medium triggered the break-down of the inert film leading to an increase in corrosion rate. This observation has been widely reported in literature /61/. It is also observed that the resistance of DSS weldment to pitting corrosion increases with the volume fraction of delta ferrite in the weld metal structure. The study affirms that pitting corrosion is structure sensitive and thrives in ferrite phases more than in austenite phases. Pitting corrosion is reported to occur by mechanisms of Cr depletion and precipitation of chromium nitride at ferrite-austenite boundaries. It was noted that the corrosion resistance of weldments increases with welding current. The study did not elucidate the influence of electrode coating basicity on the corrosion properties of DSS weld metal. Pereira et al. /56/ carried out corrosion studies on UNS S32205 DSS welded joint conducted at varied heat inputs using gas metal arc welding (GMAW) process with ER2209 filler rod. Different weld metal samples were produced by varying heat inputs (0.5, 1.0, and 3.5 kJ/mm) and intergranular and pitting corrosion studies were carried out in line with ASTM A262 and ASTM G48 practice A, respectively. The HAZ of the joints produced with high heat input (3.5 kJ/mm) has characteristic coarse austenite grain structures and were found to be more prone to intergranular corrosion along ferrite-austenite boundaries compared to 0.5 and 1.0 kJ/mm joints. The volume fraction of the ferrite phase in the fusion zone of weld metals was observed to decrease with an increase in heat input. The propensity for pitting corrosion in HAZ irrespective of the welding heat input is favoured by the presence of the ferrite phase. This assertion agrees with several studies that reported that corrosion resistance of DSS weld metal decreases with increase in ferrite content /56, 70/. Calderon-Uriszar-Aldaca et al. /68/ studied welding characteristics of DSS in a marine medium. It was reported that weld metals of 2001, 2304 and 2205 DSS material produced by autogenously tungsten inert gas welding exhibited high corrosion resistance in a chloride environment. It can be inferred from several works reviewed that:

i. DSS weld metals corrode by the mechanism of intergranular grain boundary attack, crack initiation at susceptible microstructures, chromium depletion, precipitation of carbides and nitrides and ferrite-assisted corrosion.
ii. Corrosion of DSS weld metal is microstructure sensitive with ferrite structures being more susceptible than austenite phases.
iii. Corrosion resistance of DSS weld metal increases with heat input.
iv. DSS weldments are characterized by high-temperature HAZ which exhibits more tendency to pitting corrosion than the weld metal fusion zone.
v. Fusion weld metal zones and HAZ were characterized by precipitation of chromium nitrides (CrN and Cr_2N) within the duplex structures and these precipitates served as nucleation sites for pitting corrosion.

CONCLUSIONS

The overview of previous studies on the corrosion of the duplex stainless-steel welded joints from 2015 to 2021 has led to the following conclusions:

- The corrosion disposition of DSS (UNS S32205) with various weldments in the presence of NaCl (3.5 wt.%) revealed that the face of the weld metal was more prone to corrosion, whereas the root of the weld metal was most resistant to corrosion. The presence of a precipitated intermetallic phase within the weld face was said to be responsible for the deterioration, /41/.
- The effect of Mo content in hyper duplex stainless steel was found not to influence corrosion at the weldment, rather low PREN austenite region and austenite-ferrite grain boundaries were prone to pitting and intergranular corrosion, /42/.
- Stir (friction) welded joint of the material (S32750) was found to exhibit optimal corrosion resistance in NaCl (1 M). Both the base metal and weldment shared exceptional and similar corrosion-resistant capabilities in the aforementioned corrosive medium, /43/.
- Findings have indicated that the weldment of the DSS joint produced by gas tungsten arc welding was more resistant to pitting than that produced by shielded metal arc welding, /24/.

Challenges and future research direction on the corrosion behaviour of DSS weld metal

After a thorough review of many works reported in the preceding sections, the following inference has been drawn concerning the challenges and future research direction on the corrosion of DSS weld metal:

- Contradictory positions have been made on the influence of welding heat input from 400-1050 °C on the corrosion of DSS. The authors in /1, 24/ reported that the increase in applied heat during welding improved weldment resistance to corrosion, while other authors /44/ observed the reverse trend. It is recommended that further studies be conducted to unmask the optimal heat input during welding that can make for exceptional resistance to the corrosion of weldment in a corrosive medium.
- There is limited information about the prediction of any variable concerning other independent variables that may have influenced the degradation of the welded DSS joint. It is recommended that predictive modelling protocols be employed to forecast the corrosion rate (dependent variable) of the welded joint based on the influence of some independent variables as corrosive medium, time of exposure of test samples to the corrosive medium, heat input during welding, and other parameters. This can be accomplished by using artificial neural network (ANN) modelling technique as employed by previous studies, /45-52/.
- Efforts should be made to investigate if corrosion inhibitors obtained from plant extracts /53/ can help to prevent the weldment corrosion of DSS.

- Methods of controlling nitrogen from shielding gas and managing the corrosion susceptibility of HAZ, /72/, are expected to attract research attention in the future.

REFERENCES

1. Gunn, R.N. (Ed.), Duplex Stainless Steels: Microstructure, properties and applications, Woodhead Publishing Ltd., 2003.
2. Davis, J.R. (Ed.), Corrosion of Weldments, ASM International, Materials Park, Ohio, 2006.
3. da Silva, B.R.S., Salvio, F., dos Santos, D.S. (2015), *Hydrogen induced stress cracking in UNS S32750 super duplex stainless steel tube weld joint*, Int. J Hydr. Energy, 40(47): 17091-17101. doi: 10.1016/j.ijhydene.2015.08.028
4. Zhao, H., Zhang, Z., Zhang, H., et al. (2016), *Effect of ageing time on intergranular corrosion behavior of a newly developed LDX 2404 lean duplex stainless steel*, J Alloys Compounds, 672: 147-154. doi: 10.1016/j.jallcom.2016.02.101
5. Selvabharathi, R. (2019), *Effect of post weld heat treatment and TiAlSiN coating on the tensile strength of autogenous plasma arc welding of duplex/super austenitic stainless steels*, J Manuf. Proc. 38: 135-147. doi: 10.1016/j.jmapro.2019.01.008
6. Mohammed, M.A., Shrikrishna, K.A., Sathiya, P., Goel, S. (2015), *The impact of heat input on the strength, toughness, microhardness, microstructure and corrosion aspects of friction welded duplex stainless steel joints*, J Manuf. Proc. 18: 92-106. doi: 10.1016/j.jmapro.2015.01.004
7. Lage, M.A., Assis, K.S., Mattos, O.R. (2015), *Hydrogen influence on fracture toughness of the weld metal in super duplex stainless steel (UNS S32750) welded with two different heat inputs*, Int. J Hydr. Energy, 40(47): 17000-17008. doi: 10.1016/j.ijhydene.2015.07.150
8. Zhang, Z., van der Mee, V., Golding, M., et al. (2019), *Pitting corrosion resistance properties of super duplex stainless steel weld metals and influencing factors*, Welding in the World, 63 (3): 617-625. doi: 10.1007/s40194-018-00684-y
9. Bilyy, O.L., González-Sánchez, J., de León Gomez, C.A. (2021), *Effect of external electromagnetic fields on the corrosion fatigue of welded joints of 2205 duplex stainless steel*, Mater. Sci. 56: 691-696. doi: 10.1007/s11003-021-00484-8
10. Guo, Y., Sun, T., Hu, J., et al. (2016), *Microstructure evolution and pitting corrosion resistance of the Gleeble-simulated heat-affected zone of a newly developed lean duplex stainless steel 2002*, J Alloys Compounds, 658: 1031-1040. doi: 10.1016/j.jallcom.2015.10.218
11. Lv, J.-L.,, Liang, T., Wang, C., Dong, L. (2015), *Comparison of corrosion properties of passive films formed on coarse grained and ultrafine grained AISI 2205 duplex stainless steels*, J Electroanal. Chem. 757: 263-269. doi: 10.1016/j.jelechem.2015.09.036
12. IMOA, Practical Guidelines for the Fabrication of Duplex Stainless Steel, 3rd Ed., Publ. Int. Molybd. Ass., London, UK, 2014.
13. Hertzman, S., Charles, J. (2011), *On the effect of nitrogen on duplex stainless steels*, Rev. Métall. 108(7-8): 413-425. doi: 10.1051/metal/2011071
14. Brytan, Z., Niagaj, J. (2016), *Corrosion resistance and mechanical properties of TIG and A-TIG welded joints of lean duplex stainless steel S82441/1.4662*, Arch. Metall. Mater. 61(2): 771-784. doi: 10.1515/amm-2016-0131
15. Francis, R., Byrne, G. (2021), *Duplex stainless steels - Alloys for the 21st century*, Metals, 11(5): 836. doi: 10.3390/met11050836
16. Higelin, A., Le Manchet, S., Passot, G., et al. (2022), *Heat-affected zone ferrite content control of a duplex stainless steel grade to enhance weldability*, Weld. World, 66: 1503-1519. doi: 10.1007/s40194-022-01326-0
17. Smith, L.D. (2023), *Gas tungsten arc welding fundamentals: Understanding GTAW*, last accessed Dec. 4, 2023, from: https://www.thefabricator.com/thewelder/article/arcwelding/gas-tungsten-arc-welding-fundamentals-understanding-gtaw
18. Rathod, D.W., *Chapter 4 - Comprehensive analysis of gas tungsten arc welding technique for Ni-base weld overlay*, In: K. Gupta, J.P. Davim, J.P. Davim (Eds.), Advanced Welding and Deformation, Handbooks in Advanced Manufacturing, Elsevier, 2021, pp.105-126. doi: 10.1016/B978-0-12-822049-8.00004-9
19. Kuroda, T., Ikeuchi, K., Kitagawa, Y. (2005), *Microstructure control for joining advanced stainless steel*, Novel Mater. Process. Adv. Electrom. Energy Sources, Proc., Osaka, Japan, 2004: 419-422. doi: 10.1016/b978-008044504-5/50086-6
20. Geng, S., Sun, J., Guo, L., Wang, H. (2015), *Evolution of microstructure and corrosion behavior in 2205 duplex stainless steel GTA-welding joint*, J Manuf. Proc. 19: 32-37. doi: 10.1016/j.jmapro.2015.03.009
21. Moteshakker, A., Danaee, I. (2016), *Microstructure and corrosion resistance of dissimilar weld-joints between duplex stainless steel 2205 and austenitic stainless steel 316L*, J Mater. Sci. Technol. 32(3): 282-290. doi: 10.1016/j.jmst.2015.11.021
22. Lai, R., Cai, Y., Wu, Y., et al. (2016), *Influence of absorbed nitrogen on microstructure and corrosion resistance of 2205 duplex stainless steel joint processed by fiber laser welding*, J Mater. Proces. Technol. 231: 397-405. doi: 10.1016/j.jmatprotec.2016.01.016
23. dos Santos Leite, A.M., Terada, M., Pereira, V.F., et al. (2019), *On the pitting resistance of friction stir welded UNS S82441 lean duplex stainless steel*, J Mater. Res. Technol. 8(3): 3223-3233. doi: 10.1016/j.jmrt.2019.05.010
24. Elsaady, M.A., Khalifa, W., Nabil, M.A., El-Mahallawi, I.S. (2018), *Effect of prolonged temperature exposure on pitting corrosion of duplex stainless steel weld joints*, Ain Shams Eng. J, 9(4): 1407-1415. doi: 10.1016/j.asej.2016.09.001
25. Sun, K., Zeng, M., Shi, Y., Shen, X. (2018), *Microstructure and corrosion behavior of S32101 stainless steel underwater dry and wet welded joints*, J Mater. Proces. Technol. 256: 190-201. doi: 10.1016/j.jmatprotec.2018.02.018
26. Singh, J., Shahi, A.S. (2020), *Metallurgical and corrosion characterization of electron beam welded duplex stainless steel joints*, J Manuf. Proces. 50: 581-595. doi: 10.1016/j.jmapro.2020.01.009
27. de Souza, D.D.B.G., Vilarinho, L.O. (2020), *Influence of present phases in corrosion and mechanical behavior of UNS S31803 duplex stainless steel welded by conventional short circuit MIG/MAG process*, J Mater. Res. Technol. 9(5): 11244-11254. doi: 10.1016/j.jmrt.2020.08.026
28. Zhang, Y., Cheng, S., Wu, S., Cheng, F. (2020), *The evolution of microstructure and intergranular corrosion resistance of duplex stainless steel joint in multi-pass welding*, J Mater. Proces. Technol. 277: 116471. doi: 10.1016/j.jmatprotec.2019.116471
29. Ma, C.Y., Zhou, L., Zhang, R.X., et al. (2020), *Enhancement in mechanical properties and corrosion resistance of 2507 duplex stainless steel via friction stir processing*, J Mater. Res. Technol. 9(4): 8296-8305. doi: 10.1016/j.jmrt.2020.05.057
30. Ma, Q., Luo, C., Liu, S., et al. (2021), *Investigation of arc stability, microstructure evolution and corrosion resistance in underwater wet FCAW of duplex stainless steel*, J Mater. Res. Technol. 15: 5482-5495. doi: 10.1016/j.jmrt.2021.11.023
31. Nanavati, P.K., Kotecki, D.J., Soman, S.N. (2019), *Effect of weld metal ferrite content on mechanical properties and stress corrosion cracking resistance in 22 Cr 5 Ni duplex stainless steel*, Weld. World, 63: 793-805. doi: 10.1007/s40194-019-00708-1
32. Alwin, B., Lakshminarayanan, A.K., Vasudevan, M., Vasantharaja, P. (2017), *Assessment of stress corrosion cracking resistance of activated tungsten inert gas-welded duplex stainless steel joints*, J Mater. Eng. Perform. 26(12): 5825-5836. doi: 10.1007/s11665-017-3057-0

33. Singh, S., Singh, J., Shahi, A.S. (2020), *Investigation on aging-induced degradation of impact toughness and corrosion performance of duplex stainless steel weldment*, Trans. Ind. Inst. Metals, 73(11): 2747-2765. doi: 10.1007/s12666-020-02070-z
34. Kangazian, J., Shamanian, M. (2019), *Effect of pulsed current on the microstructure, mechanical properties and corrosion behavior of Ni-based alloy/super duplex stainless steel dissimilar welds*, Trans. Ind. Inst. Metals, 72: 2403-2416. doi: 10.1007/s12666-019-01693-1
35. Gupta, A., Kumar, A., Baskaran, T., et al. (2018), *Effect of heat input on microstructure and corrosion behavior of duplex stainless steel shielded metal arc welds*, Trans. Indian Inst. Metals, 71(7): 1595-1606. doi: 10.1007/s12666-018-1294-z
36. da Cruz Junior, E.J., Gallego, J., Settimi, A.G., et al. (2021), *Influence of nickel on the microstructure, mechanical properties, and corrosion resistance of laser-welded super-duplex stainless steel*, J Mater. Eng. Perform. 30(4): 3024-3032. doi: 10.1007/s11665-021-05590-x
37. Wu, M., Liu, F., Pu, J., et al. (2017), *The microstructure and pitting resistance of weld joints of 2205 duplex stainless steel*, J Mater. Eng. Perform. 26(11): 5341-5347. doi: 10.1007/s11665-017-2976-0
38. Hu, Y., Shi, Y., Shen, X., Wang, Z. (2018), *Microstructure evolution and selective corrosion resistance in underwater multi-pass 2101 duplex stainless steel welding joints*, Metall. Mater. Trans. A, 49(8): 3306-3320. doi: 10.1007/s11661-018-4686-0
39. Júnior, R.C., Esteves, L., Santos, N.F., et al. (2019), *Influence of heat input and cold wire feeding rate on pitting corrosion resistance of submerged arc welding duplex stainless steel welds*, J Mater. Eng. Perform. 28(4): 1969-1976. doi: 10.1007/s11665-019-03967-7
40. Atapour, M., Sarlak, H., Esmailzadeh, M. (2015), *Pitting corrosion susceptibility of friction stir welded lean duplex stainless steel joints*, The Int. J Adv. Manuf. Technol. 83(5-8): 721-728. doi: 10.1007/s00170-015-7601-5
41. Tümer, M., Mert, T., Karahan, T. (2021), *Investigation of microstructure, mechanical, and corrosion behavior of nickel-based alloy 625/duplex stainless steel UNS S32205 dissimilar weldments using ERNiCrMo-3 filler metal*, Weld. World, 65: 171-182. doi: 10.1007/s40194-020-01011-0
42. Kim, N., Gil, W., Lim, H., et al. (2019), *Variation of mechanical properties and corrosion properties with Mo contents of hyper duplex stainless-steel welds*, Metals Mater. Int. 25(1): 193-206. doi: 10.1007/s12540-018-0166-8
43. Santa Cruz, L.A., Marques, I.J., Urtiga Filho, S.L., et al. (2019), *Corrosion evaluation of duplex and superduplex stainless steel friction stir welds using potentiodynamic measurements and immersion tests in chloride environments*, Metallogr. Microstr. Anal. 8: 32-44. doi: 10.1007/s13632-018-0506-6
44. Ouali, N., Khenfer, K., Belkessa, B., et al. (2019), *Effect of heat input on microstructure, residual stress, and corrosion resistance of UNS 32101 lean duplex stainless steel weld joints*, J Mater. Eng. Perform. 28: 4252-4264. doi: 10.1007/s11665-019-0194-w
45. Ndukwe, A.I., Umoh, S., Ugwochi, C., et al. (2022), *Prediction of compression strength of bamboo reinforced low-density polyethylene waste (LDPEw) composites*, Compos. Theory Pract. 22 (3): 142-149.
46. Ndukwe, A.I., Anyakwo, C.N. (2017), *Modelling of corrosion inhibition of mild steel in hydrochloric acid by crushed leaves of sida acuta (Malvaceae)*, The Int. J Eng. Sci. (IJES), 6(1): 22-33.
47. Ndukwe, A.I., Anyakwo, C.N. (2017), *Predictive model for corrosion inhibition of mild steel in HCl by crushed leaves of clerodendrum splendens*, Int. Res. J Eng. Technol. (IJRET), 4 (2): 679-688.
48. Ndukwe, A.I., Anyakwo, C.N. (2017), *Modelling of corrosion inhibition of mild steel in sulphuric acid by thoroughly crushed leaves of voacanga africana (Apocynaceae)*, Amer. J Eng. Res. 6(1): 344-356.
49. Ndukwe, A.I., Anyakwo, C.N. (2017), *Corrosion inhibition model for mild steel in sulphuric acid by crushed leaves of clerodendrum splendens (Verbenaceae)*, Int. J Sci. Eng. Appl. Sci. 3(3): 39-49.
50. Anyakwo, C.N., Ndukwe, A.I. (2017), *Mathematical model for corrosion inhibition of mild steel in hydrochloric acid by crushed leaves of tridax procumbens (Asteraceae)*, Int. J Sci. Eng. Investig. 6(65): 81-89.
51. Anyakwo, C.N., Ndukwe, A.I. (2017), *Prognostic model for corrosion-inhibition of mild steel in hydrochloric acid by crushed leaves of voacanga africana*, Int. J Comput. Theor. Chem. 5(3): 30-41. doi: 10.11648/j.ijctc.20170503.12
52. Ndukwe, A.I., Anyakwo, C.N. (2017), *Predictive corrosion-inhibition model for mild steel in sulphuric acid (H_2SO_4) by leaf-pastes of sida acuta plant*, J Civil, Constr. Environm. Eng. 2(5): 123-133. doi: 10.11648/j.jccee.20170205.11
53. Ndukwe, A.I. (2022), *Green inhibitors for corrosion of metals in acidic media: A review*, Acad. J Manuf. Eng. 20(2): 36-50.
54. Omiogbemi, I.M.B., Yawas, D.S., Das, A., et al. (2022), *Mechanical properties and corrosion behaviour of duplex stainless steel weldment using novel electrodes*, Sci. Rep. 12: 22405. doi: 10.1038/s41598-022-26974-6
55. Hou, Y., Nakamori, Y., Kadoi, K., et al. (2022), *Initiation mechanism of pitting corrosion in the weld heat affected zone of duplex stainless steel*, Corr. Sci. 201: 110278. doi: 10.1016/j.corsci.2022.110278
56. Pereira, H.B., Moreira. M.F., Almeida, N.L., Batista, I.P. (2019), *Influence of stress and temperature on stress corrosion cracking of welded duplex stainless steel joints under drop evaporation test*, In: NACE Int. CORROSION Conf. 2019, Tennessee, USA. Proceedings, USA: OnePetro; 2019.
57. Shen, K., Jiang, W., Sun, C., et al. (2022), *Unlocking the influence of microstructural evolution on hardness and pitting corrosion in duplex stainless welded joints*, Corr. Sci. 206: 110532. doi: 10.1016/j.corsci.2022.110532
58. Singh, J., Shahi, A.S. (2022), *Microstructure and corrosion behavior of duplex stainless steel electron beam welded joint*, J Mater. Sci. 57: 9454-9479. doi: 10.1007/s10853-022-07241-5
59. Nuñez de la Rosa, Y.E., Calabokis, O.P., Uris, G.M.P., Borges, P.C. (2022), *Pitting and crevice corrosion behavior of the duplex stainless steel UNS S32205 welded by using the GTAW process*, Mat. Res. 25: e20220179. doi: 10.1590/1980-5373-MR-2022-0179
60. Cui, S., Pang, S., Pang, D., et al. (2023), *The microstructure and pitting corrosion behavior of K-TIG welded joints of the UNS S32101 duplex stainless steel*, Materials, 16(1): 250. doi: 10.3390/ma16010250
61. Miranda-Pérez, A.F., Rodríguez-Vargas, B.R., Calliari, I., Pezzato, L. (2023), *Corrosion resistance of GMAW duplex stainless steels welds*, Materials, 23; 16(5): 1847. doi: 10.3390/ma16051847
62. Verma, J., Taiwade, R.V. (2017), *Effect of welding processes and conditions on the microstructure, mechanical properties and corrosion resistance of duplex stainless steel weldments - A review*, J Manuf. Proc. 25: 134-152. doi: 10.1016/j.jmapro.2016.11.003
63. Kotecki, D.J., Siewert, T.A. (1992), *WRC-1992 constitution diagram for stainless steel weld metals: a modification of the WRC-1988 diagram*, Weld. Res. Suppl. Weld. J, 71: 171s-177s.
64. Baldev, R., Shankar, V., Bhaduri, A.K., Welding Technology for Engineers, Narosa Publ. House, New Delhi, India, 2006.
65. Di, X., Zhong, Z., Deng, C., et al. (2016), *Microstructural evolution of transition zone of clad X70 with duplex stainless steel*, Mater. Des. 95: 231-236. doi: 10.1016/j.matdes.2016.01.087

66. Mohammed, G.R., Ishak, M., Aqida, S.N., Abdulhadi, H.A. (2017), *Effects of heat input on microstructure, corrosion and mechanical characteristics of welded austenitic and duplex stainless steels: a review*, Metals, 7(2): 39. doi: 10.3390/met7020039
67. dos Santos, N.F., Esteves, L., Garcia, J.H.N., et al. (2020), *Microstructural and corrosion resistance of lean duplex stainless steel UNS S32304 welded by SAW with cold wire addition*, Corrosion, 76(7): 619-627. doi: 10.5006/3468
68. Calderon-Uriszar-Aldaca, I., Briz, E., García, H., Matanza, A. (2020), *The weldability of duplex stainless-steel in structural components to withstand corrosive marine environments*, Metals, 10(11): 1475. doi: 10.3390/met10111475
69. Chen, R., Jiang, P., Shao, X., Mi, G., Wang, C. (2017), *Effect of the magnetic field applied during laser-arc hybrid welding in improving the pitting resistance of the welded zone in austenitic stainless steel*, Corros. Sci. 126: 385-391. doi: 10.1016/j.corsci.2017.07.019
70. Gennari, C., Lago, M., Bögre, B., et al. (2018), *Microstructural and corrosion properties of cold rolled laser welded UNS S32750 duplex stainless steel*, Metals, 8(12): 1074. doi: 10.3390/met8121074
71. Calabokis, P.O., Núñez de la Rosa, Y., Lepienski, C.M., et al. (2021), *Crevice and pitting corrosion of low-temperature plasma nitrided UNS S32750 super duplex stainless steel*, Surf. Coat. Technol. 413: 127095. doi: 10.1016/j.surfcoat.2021.127095
72. Ramesh, A., Kumar, V., Anuj, P., Khanna, P. (2021), *Weldability of duplex stainless steels - A review*, E3S Web of Conf. 309: 01076. doi: 10.1051/e3sconf/202130901076
73. Zhang, Z., Jing, H., Xu, L., et al. (2018), *Effect of post-weld heat treatment on microstructure evolution and pitting corrosion resistance of electron beam-welded duplex stainless steel*, Corr. Sci. 141: 30-45. doi: 10.1016/j.corsci.2018.06.030
74. Torres, C., Johnsen, R., Iannuzzi, M. (2021), *Crevice corrosion of solution annealed 25Cr duplex stainless steels: Effect of W on critical temperatures*, Corros. Sci. 178: 109053. doi: 10.1016/j.corsci.2020.109053
75. Pereira, H.B., Pimentel, T.H.C., Alberto da Silva, C., et al. (2022), *Influence of welding energy on intergranular and pitting corrosion susceptibility of UNS S32205 duplex stainless-steel joints*, Mater. Res. 25(s1): e20210488. doi: 10.1590/1980-5373-MR-2021-0488